Thermal, biodegradation and theoretical perspectives on nanoscale confinement in starch/cellulose nanocomposite modified via green crosslinker

Preetha Balakrishnan, V.G. Geethamma, Sreerag Gopi, Martin Georges Thomas, Matjaž Kunaver, Miroslav Huskić, Nandakumar Kalarikkal, Tatiana Volova, Didier Rouxel, Sabu Thomas

Thermal, biodegradation and theoretical perspectives on nanoscale confinement in starch/cellulose nanocomposite modified via green crosslinker

Preetha Balakrishnan, V.G. Geethamma, Sreerag Gopi, Martin George Thomas, Matjaž Kunaver, Miroslav Huskić, Nandakumar Kalarikkal, TatianaVolova, Didier Rouxel, Sabu Thomas

https://doi.org/10.1016/j.ijbiomac.2019.05.088Get rights and content

Preetha Balakrishnana, V.G. Geethammaa,SreeragGopib, Martin George Thomasc,MatjažKunaverd,Miroslav Huskićd,e, Nandakumar Kalarikkala,TatianaVolovaf, Didier Rouxelg, Sabu Thomas
,f,g,h,□aInternational and Inter University Center for Nanoscience and Nanotechnology, Mahatma Gandhi University, Kottayam, Kerala 686560, IndiabDepartment of Research and Development, ADSO Naturals Pvt. Ltd., 2/5, RMV Second Stage, Bangalore, Karnataka 560094, IndiacUniversity of Pau and Pays de l'Adour IPREM - UMR 5254 UPPA/CNRS–EPCP, Technopole Helioparc - 2, av. Pdt P. Angot, 64 053 PAU Cedex 09, FrancedNational Institute of Chemistry, Department of Polymer Chemistry and Technology, Hajdrihova 19, SI-1000 Ljubljana, SloveniaeFaculty for Polymer Technology, Ozare 19, 2380 Slovenj Gradec, SloveniafSiberian Federal University, 79 Svobodnyi Av., Krasnoyarsk 660041, RussiagUMR CNRS 7198 - Université de Lorraine, FrancehSchool of Chemical Sciences, Mahatma Gandhi University, Kottayam, Kerala 686560, Indiaabstractarticle infoArticle history

Thomas).https://doi.org/10.1016/j.ijbiomac.2019.05.0880141-8130/Contents lists available atScienceDirectInternational Journal of Biological Macromoleculesjournal homepage:http://www.elsevier.com/locate/ijbiomac

Abstract

In this research work, we propose a synergistic effect of a green crosslinker and cellulose nanomaterial on the crystallinity, viscoelastic, and thermal properties of starch nanocomposites. A disaccharide derivative was used as a bio crosslinker and nanofiber from pineapple leaf as a reinforcing phase for starch. Sucrose was oxidised using periodate, that can selectively oxidise the vicinal hydroxyl group of sucrose and form tetra aldehyde derivative. Crystallinity of films after crosslinking decreased with successive addition of crosslinker. The melting temperature of films increased because of formation of more dense structure after crosslinking. Morphological investigations were analysed by atomic force microscopy. Polymer chain confinement and mechanics were quantified. The crosslink densities of the films were calculated using two models, phantom model and affine model, using storage modulus data. By using very low amount of crosslinker and nanoreinforcement, the properties of thermoplastic starch were significantly improved.

Graphical abstract

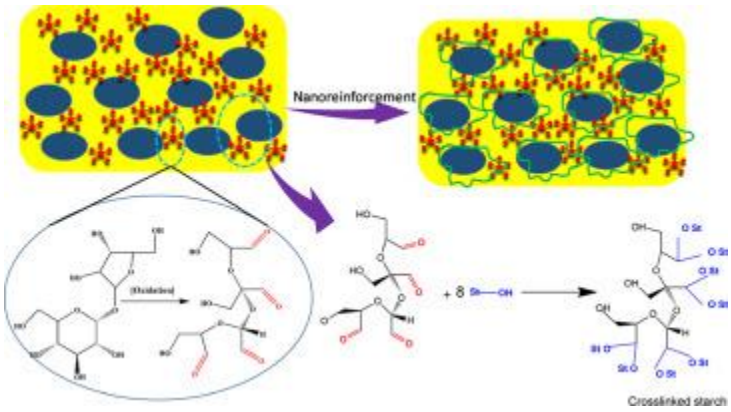

1. Download high-res image (183KB)
2. Download full-size image

Keywords

Crosslinking
Cellulose nanofiber
Viscoelastic

1. Introduction

In the creation of high performance advanced polymer nanocomposites, various nanosized fillers are used as reinforcing material. Fine dispersion of nanoparticle within the polymer matrix leads to high performance composites due to high interfacial area which is in the range of molecular dimensions [1].

Starch is one of the most investigated biodegradable materials obtained from renewable resources. It is a resourceful polysaccharide with various positive points like low price, availability, use in food and non-food industry etc. Native starch occurs in the form of distinct and semi-crystalline microscopic granules held together by network of its associated molecules [2]. At present starch has received much attention because of depletion of petroleum fuels and serious environmental and health issues associated with the disposal of petroleum derived materials. Starch is not truly thermoplastic in nature but can be converted into one, using water and non-aqueous volatile materials called plasticizers (generally polyols like glycerol). However, the hygroscopic nature of starch limits its applications. Also, in addition, retrogradation and crystallization of mobile starch phase leads to change in its thermomechanical properties. Starch is immiscible with other commonly used polymers due to its highly polar nature. Reinforcing with cellulosic fillers in thermoplastic starch improves its property by preserving the biodegradability.

There are several methods reported so far to improve the performance of starch based composites like blending [[3], [4], [5], [6], [7]], crosslinking [[8], [9], [10]], micro and nanoreinforcement, [[11], [12], [13]] etc. Crosslinking is one of the most efficient methods to improve the properties of starch-based system. But at the same time most of the crosslinkers are incompatible with starch, costly and even carcinogenic [14,15]. Starch crosslinked with boric acid [16], citric acid [17] etc. are widely reported.

The importance of the dynamic mechanical analysis as a tool to investigate the performance of composite is very dominant. It has been proven to be one of the most efficient methods to study

the behaviour of materials under various conditions. For starch based composite system, there is a general difficulty in interpreting the mechanical property of the system, which may be due to the existence of different type of relaxation arising from various constituents like starch (amylopectin), glycerol, water and nonreinforcement [2,18,19]. For e.g. Butler et al. [20] proposed possible causes of secondary relaxation in starch system, that may be noted as (1) rotation of polysaccharide hydroxyl groups (2), rotation of methylol group (3), localized motion of chain backbone about (1-6)-α linkage of glycerol group and finally the possibility of boat and chair confirmation and conversion of glucose unit. The hydroxyl group of water molecules reacts with the hydroxyl group of the polysaccharide (starch) which leads to much strong and turgid hydrogen bonded network than that of other polymers [21].

There are few research works on the effect of periodate oxidation on starches from various botanical origin. Veelaert et al. [22] studied the structural and physicochemical changes associated with the periodate cleavage of potato starch. They found that at lower degree of oxidation, the structural disruption of starch granules resulted in the increased water sorption. But at the same time at higher oxidation content, water sorption is minimized due to the introduction of hydrophobic hemiacetal groups produced as a result of crosslinking. The presence of carbonyl groups and hemi acetal groups, shifts the gelation temperature of dialdehyde starch to higher temperature and causes a loss in crystallinity [23].

In our previous report the dynamics and confinement of starch/cellulose nanofiber system without the presence of crosslinker were studied [19]. In this paper, the starch films were crosslinked with oxidised sucrose, a green crosslinker, to improve the final performance of nanocomposite films. The studies of the nanodynamics and chain confinement of crosslinked nanocomposite films, to the best of our knowledge, such an attempt has not been reported.

2. Materials and methods

Corn starch (containing approx. 73% of amylopectin and 27% of amylose), sucrose (average molar weight of 342.49 g mol^{-1}), glycerol ($C_3H_8O_3$, molar weight of 92.09 $gmol^{-1}$), sodium periodate and potassium chloride were purchased from Sigma Aldrich and used without any further purification. Cellulose nanofibrils (CNFs) of about 20–50 nm in diameter and up to several μm in length was obtained from pineapple leaf fiber as earlier reported [19]. Milli Q water was used for solution casting.

2.1. Preparation of oxidised sucrose (OS)

The oxidised sucrose was obtained via periodate cleavage, using the procedure from Xu et al. [24] with some minor modifications. Particularly, periodate treatment was carried out to selectively oxidise vicinal hydroxyl groups. For oxidation reaction, 10 g of sucrose was mixed with 15 g of sodium periodate in 300 ml distilled water. The solution was stirred for 24 h at room temperature before 7 g of potassium chloride was added, followed by stirring for another hour at 5 °C until complete precipitation. The solution was then filtered with cheesecloth to obtain the liquid, which was a polyaldehyde of sucrose. The oxidised sucrose of around 7 wt% and pH 2.5 was stored in a refrigerator for further use.

2.2. Preparation of nanocomposite films

For the reference film, a 10 g of starch was mixed with 30 wt% of glycerol, based on the dry weight of starch, and dispersed in 100 ml distilled water by heating at 90 °C and stirring with a magnetic stirrer for 30 min. The resulting viscous solution was poured into levelled Petri dishes

and kept at room temperature for about 72 h [19] to get them fully dried. Crosslinked films were prepared by varying concentrations of oxidised sucrose such as 1, 2, and 3 wt% (based on the dry weight of starch). The same procedure was used to prepare crosslinked nanocomposite films with the addition of 5 wt% of CNF dispersions to the crosslink solutions. The films were dried in an oven at 50 °C for 24 h to allow complete crosslinking

3. Characterizing techniques

3.1. Fourier Transform Infrared Spectroscopic (FTIR) analysis

FTIR analysis was performed by a Perkin-Elmer spectrometer with a golden gate ATR accessory attached to a diamond crystal. The spectra were recorded in ambient condition from 16 scans at the resolution of 4 cm^{-1} within the region of 4000–100 cm^{-1}. Before the analysis, the samples were conditioned at 50 ± 2 °C for 45 min, to ensure no moisture adherence to the sample.

3.2. X-Ray Diffraction (XRD) analysis

Crystallinity of the nanocomposite was determined by XRD measurement on a Bruker powder diffractometer. Prior to the experiments the composite films were dried in an oven overnight at a temperature of 50 °C to avoid any adhering moisture. Radial scans of intensity were recorded over scattering 2θ angles from 5 to 55° (step size = 0.02°, scanning rate = 2 s/step) using a Ni-filtered Cu K radiation (θ = 1.5406 Å) an operating voltage of 45 kV, and a filament current of 40 mA.

3.3. Differential scanning colorimetry (DSC)

For DSC measurements, an amount of approximately 5 mg of the sample was placed in an aluminum pan and measured in the temperature range of −40 °C to 250 °C during both, heating and cooling cycles, with a rate of 10 °C/min. The measurements were performed using a Q200 (TA) calorimeter under Helium purge.

3.4. Atomic force microscopy (AFM)

Atomic force microscopy was performed using an APER-A-100 SPM. Tapping mode was used to capture images. Thin pieces of the films were dried in an air circulating oven for about 3 h at 50 °C, to avoid any moisture adhering into the sample surface.

3.5. Dynamic mechanical analysis (DMA)

Dynamic mechanical analysis was performed on a TA Q800 thermal analyzer (Q800 DMA) using a thin film clamp. The viscoelastic properties were measured at a frequency of 1 Hz, strain amplitude of 5 μm in a temperature range −120 °C to 70 °C. The heating rate was 2 °C/min.

3.6. Biodegradability analysis

The starch nanocomposite specimen of dimension 40 mm × 8 mm × 2 mm were buried at about 10 cm depth in a mixture of equal ratio of sand and soil in Kottayam, Kerala, India. The samples were then kept at ambient temperature. Water was supplied at the intervals of 2 days so as to keep the soil moist all day. Each specimen then dug out of the soil after a specific interval of each day for one month. After every fixed period, samples were carefully cleaned with distilled

water before being dried at 50 °C for 24 h and then weighed to determine the weight loss using the following equation:

(1)
where, Mi and Mf respectively are initial mass and final mass.

4. Results and discussions

4.1. Structural characterization

Fig. 1A shows the spectra of both native and modified sucrose. Both spectra had a characteristic peak at 3000–3500 cm^{-1} which corresponds to the hydroxyl (O—H) stretching vibration, and a duplet peak between 2820 and 3000 cm-1 due to the C—H stretching related to aldehydes and the alkyl chain, respectively. The absorbance intensity at 3200–3500 cm^{-1} band in the spectrum of OS sample is much lower and broaden, indicating a strong interaction of hydroxy groups of sucrose with the periodate. This results decrease in the amount of hydroxyl groups by their conversion into their aldehyde derivatives [25], which can be seen by a new peak appeared at about 1646 cm-1 for OS sample corresponding to the conjugated stretching vibration of the aldehyde (C=O) groups. Also, the intensity of peak at 3200–3500 cm^{-1} corresponds to the hydroxyl group decreases which might be due to the conversion of hydroxyl groups to aldehyde group during modification reaction.

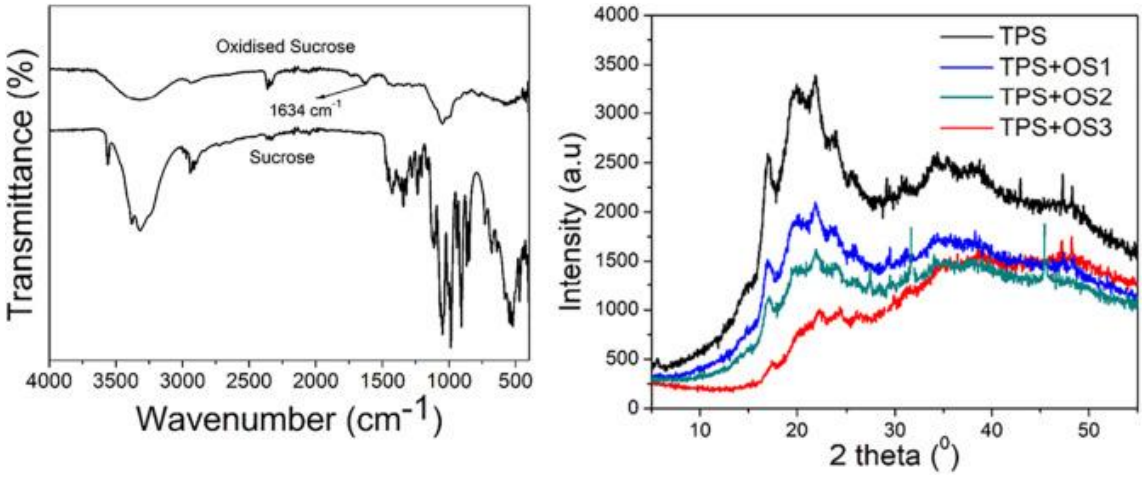

1. Download high-res image (184KB)
2. Download full-size image

Fig. 1. (A): FTIR spectra of sucrose and modified sucrose. (B) XRD diffractogram of crosslinked starch films with different OS content.

4.2. Crystallinity of nanocomposite films

Crystallinity of composite films was characterized using XRD (Fig. 1B). Starch is semi-crystalline in nature. But during the processing of thermoplastic starch, due to thermal and physical forces the starch granules swell and burst out above their gelation temperature [26]. After storage, the linear amylopectin tends to recrystallize and material changes to semi-crystalline again. Yu et al. studied the crystalline nature of thermoplastic dialdehyde starch and found that during the oxidation of starch using periodate, it oxidises the crystalline regions of starch and degrades the amorphous fraction [27]. This will lead to lower the crystallinity of samples after successive periodate concentration.

The crystallinity of crosslinked samples decreases with increase in crosslink content. Typically starch exhibits three types of diffraction; A-type, B-type and C-type (combination of A and B type). Corn starch exhibit A-type crystallinity with 2Θ angles at 15°, 17°, and around 23° [28]. All films show characteristic peaks at the same region and intensity of the peaks decreases gradually. This may be due to the disruption of long range order of starch macromolecular chain as a result of crosslinking with OS. When OS is used as a crosslinker for starch, the aldehyde group of OS, reacts with the hydroxyl group of starch to form acetal linkages. Also, the crosslinking primarily effects the crystalline regions of thermoplastic starch and leads to decrease in crystallinity of the samples.

4.3. Atomic force microscopy

AFM images of surface characteristics of starch nanocomposite films are shown in Fig. 2. Fig. 2(A) shows the morphology of neat thermoplastic starch (TPS) without crosslinker and nanoreinforcement. It has a heterogeneous surface with amorphous nature. The AFM pictures Fig. 2(B to G) show a multi-phased system and there is an indication through the phase images that one of the phases is forming a network in the second phase with a relatively homogeneous distribution of the phases [29]. Fig. 2(B, D and F) shows that starch films crosslinked with 1, 2 and 3 wt% oxidised sucrose. The figures show the TPS films were modified and existence of two phases was visible. Upon the addition of 5 wt% CNF, Fig. 2(C, E and G) into the crosslinked films, the roughness of the films increases, and existence of homogenous hills and heaps indicates the dispersion of CNF into the crosslink samples. Also, roughness of the films increases with the nanoreinforcement.

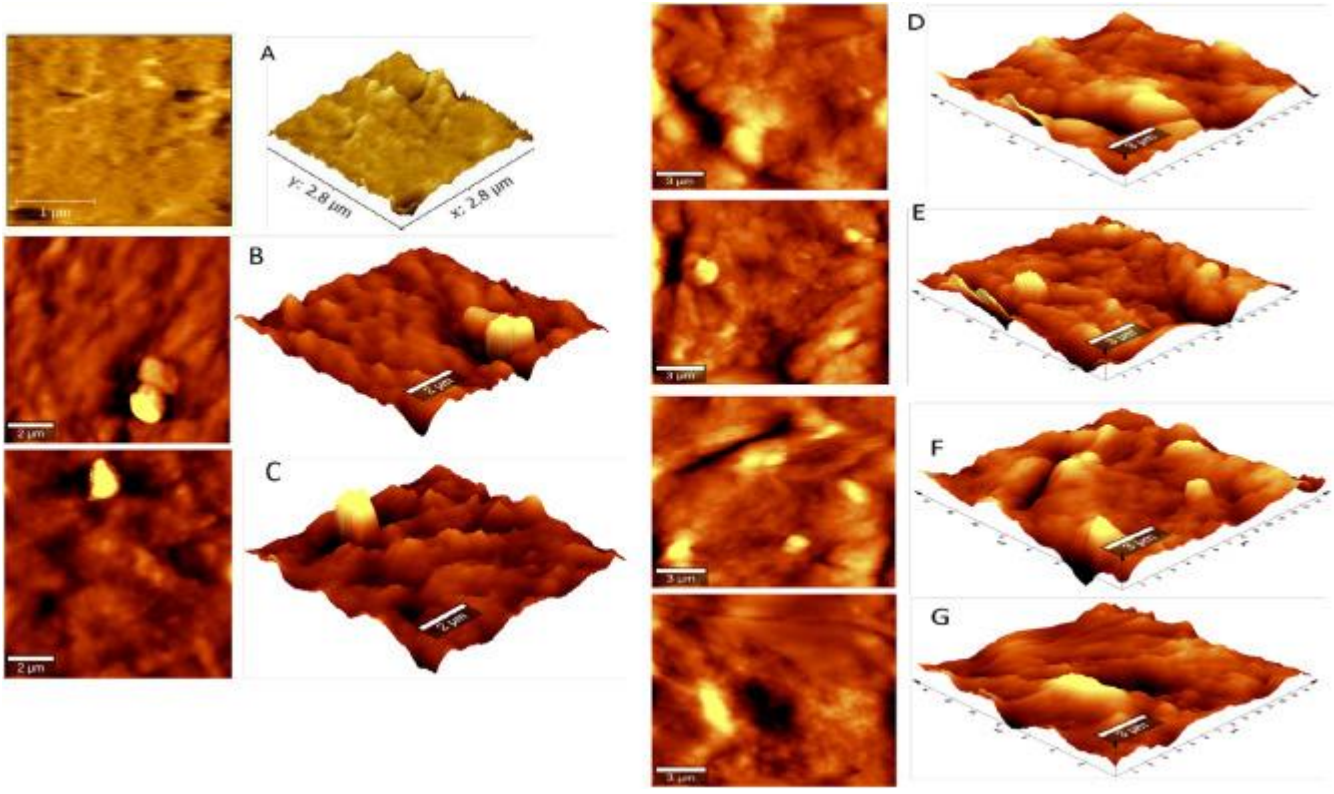

1. Download high-res image (451KB)
2. Download full-size image

Fig. 2. AFM images of crosslinked films and crosslinked nanocomposite films (A) neat TPS, (B) TPS + OS1, (C) TPS + OS1/CNF5, (D) TPS + OS2, (E) TPS + OS2/CNF5, (F) TPS + OS3, (G) TPS + OS3/CNF5.

4.4. Thermal analysis

Differential scanning colorimetry (DSC) is an important tool to investigate the amount of heat absorbed or released when the material is subjected to physical or chemical changes. DSC thermograms of crosslinked and un-crosslinked films are shown in Fig. 3.

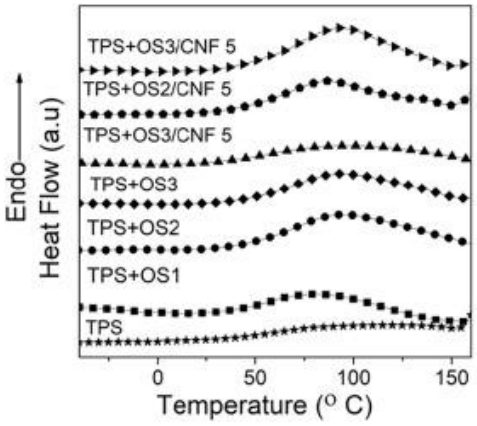

Sample	Melting Temperature Tm (°C)
TPS	71.5
TPS+OS1	79.5
TPS+OS2	90.5
TPS+OS3	94.8
TPS+OS1/CNF5	85.0
TPS+OS2/CNF5	86.8
TPS+OS3/CNF5	92.4

1. Download high-res image (136KB)
2. Download full-size image

Fig. 3. DSC thermogram of crosslinked (second heating scan) films and crosslink nanocomposite films.

In neat TPS there is an endothermic peak at 71.5 °C. After crosslinking the endothermic peak shifts to higher temperature and also the peak changes to sharp one. For neat TPS, the endothermic peak was not clearly identifiable which was explained as melting with decomposition by Van Soest et al. [30]. But after crosslinking with OS, additional bonds are formed by crosslinking between aldehyde group of OS and hydroxyl group of TPS, increases the melting point and more sharp melting peak may result from more perfect structure, nucleation effect and the presence of crosslinks in the intercrystalline amorphous regions. This may be also due to the formation of more compact and well-defined structure [31]. The endothermic peak of crosslink samples were sharper than neat TPS, perhaps increase in stability of molecule due to hemi acetal crosslinking [23].

Unlike other amorphous polymers, in this case, in DSC investigation, starch didn't exhibit a clear Tg due to the following factors (1) crystalline fractions that surrounds the amorphous region (2) presence of moisture due to large amount of hydroxyl groups (3) intramolecular hydrogen bonding existing between the molecules (4) intercrystallite phase that mimics its original thermal behaviour. Low glass transition of starch based system are due to the presence of plasticizers (in this case glycerol), that penetrates in between the polymer chains that decreases the polar attraction of adjacent chains [32]. Properties of PVA/Starch blends crosslinked with borax were earlier reported by Sreedhar et al. [33]. Since PVA and starch can form hydrogen bonds, a specific interaction can be expected in between the crosslink and blend that results in the decrease in Tg. Table 1 shows the melting peak of samples. From table, it is clear that the melting temperature increases with increase in the crosslinker content. But after the addition of cellulose nanofibers, the melting peak found to be decrease slightly. Interfacial adhesion between the matrix and reinforcing phase at higher filler dispersion hinders to some extent the lateral rearrangements of starch polymer chains and hence crystallization of these materials [34].

4.5. Dynamic mechanical analysis

Dynamic mechanical analysis is an important tool to investigate the viscoelastic behaviour of polymeric materials. Polymers are viscoelastic in nature which comprises of both viscous and elastic components. Storage modulus is related to the amount of energy stored per cycle. Loss modulus is the amount of energy dissipated as a heat. These parameters vary upon various parameters like crosslinking, nanoreinforcement, blending etc. Tan delta is the ratio of loss to storage modulus. It's a measure of energy loss that can be expressed in terms of recoverable energy.

4.5.1. Effect on crosslinking on viscoelastic behaviour of starch nanocomposite films

Glycerol plasticized starch nanocomposite system were intricate due to the presence of four components; starch, main plasticizer glycerol, water and nanofiller. Complex interactions between these components lead to more complex behaviour of starch films in thermos-mechanical experiments. As we reported earlier starch nanocomposite reinforced with cellulose nanofiber is a heterogeneous system which consist of two regions, glycerol rich region and amylopectin region. Accumulation of glycerol and water (plasticizers) in the cellulose/amylopectin interface was earlier reported by Angles et al. [35]. The specific behaviour of amylopectin chain located near the interface probably led to a transcrystallization behaviour of amylose on the surface of cellulose nanofibers.

In this case, starch composite films were crosslinked with 1, 2 and 3 wt% of oxidised sucrose. The crosslink density of samples has a marked effect on elastic modulus at the temperature lower than the glass transition temperature [8]. The storage modulus of composite increased with increasing crosslinker content as evident from Fig. 4, due to increase in crosslink density. At lower temperature, chemical crosslinks prevent molecules from moving. Upon gradually increasing the temperature (rubbery region), the storage modulus was found to be almost the same since at higher temperature, polymer chains became mobile and temperature effect will be more profound than crosslinking effect.

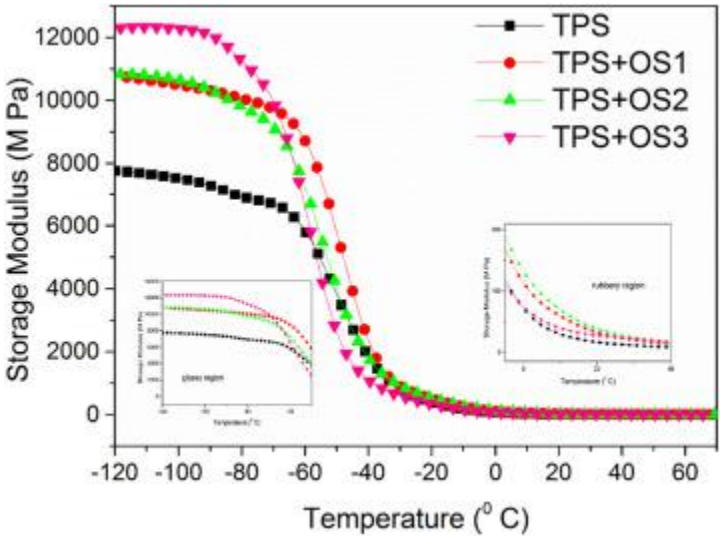

1. Download high-res image (213KB)
2. Download full-size image

Fig. 4. Plot of storage modulus Vs temperature for crosslinked films at 1 Hz frequency.

In case of unfilled matrix, starch matrix appears to be a complex heterogeneous system consisting of glycerol rich domains dispersed in amylopectin rich continues phase. Each phase exhibits its own glass transition temperature.

Loss modulus peak area is the amount of energy degenerate per cycle. Loss modulus of the crosslinked films (Fig. 5A) found to be decreasing gradually as the crosslink density increases. This is because after the crosslinking polymeric chains with much restricted mobility are obtained. Fig. 6B shows the tan delta vs temperature plot of uncrosslinked starch and crosslinked starch films. Unfilled starch matrix is a combination of glycerol rich domains dispersed in amylopectin rich continuous phase. Each phase exhibits its own glass transition, a low temperature relaxation α_1 corresponds to glycerol rich area and a high temperature relaxation α_2, corresponds to starch rich areas (amylopectin). The drop in the modulus corresponds to energy dissipation phenomenon that involves co-operative motion of long amorphous amylopectin chain rotate and translate energy. In the glycerol rich area, the height of tan delta remains almost same. Height of tan delta peak implies the effective bonding. In the glycerol rich area, due to plasticization effect, glycerol effect became more prominent than crosslinking effect. In contrast, at amylopectin rich area (glycerol lean area), tan delta peak height decreases with increasing crosslinking content. This may be due to restricted mobility of polymeric chain due to increase in crosslink content. The damping height decrease for the crosslink films implies better crosslinking of oxidised sucrose to the thermoplastic starch matrix due to the restriction in chain mobility of the starch macromolecular chain after the reaction between the aldehyde group of oxidised sucrose, the crosslinker and hydroxyl group of starch. Also, the shift of tan δ to the lower temperature of crosslink samples is primarily because of the preferential migration of plasticizing glycerol. We can also determine how varying the crosslink effects the sample network structure by examining the tan delta plot. Usually an increase in crosslink density affects the tan delta curve in three possible ways. (1) Tan delta peak shifts gradually to high temperature region because with increase in crosslink density increases the glass transition temperature (restricted chain mobility) (2) tan delta peak height will decrease with increase in crosslinker content because crosslink samples have larger elastic moduli compared to viscous moduli (3) broadening of tan delta peak. This specific effect is attributed to the increase in distribution of molecular weights between crosslinks or an increase in heterogeneity of network structure [36]. In our case, α_1 relaxation shifted towards lower temperature as shown in Table 2. This decrease in Tg is attributed to the migration of plasticizer in between the polymer chains that increases the flexibility of chain backbone. The theoretical crosslink densities can be calculated by various methods. We can obtain approximate crosslink density of the crosslinked samples from dynamic mechanical analysis. To do the same, we assume the system to obey the theory of rubber elasticity [37]. One form of this theory gives the equilibrium shear modulus *G* as

(2)υ

where, υ concentration of elasticity of active chain, h the empirical parameter and its values ranges from 0 to 1, μ is the concentration of elastically active junctions. R is the gas constant and T the temperature in kelvin. In a perfect network with functionality *f*, μ is equal to 2υ/*f*. in this case, we assume that only chemical crosslinking effects and contributes to the modulus of system and neglect the contribution from physical entanglements. Physical entanglements can be accounted for by adding the term $G^{\circ}_{N}T_e$ to the right side of Eq. (2), where $G^{\circ}N$ is the plateau modulus associated with physical entanglements in a non-chemically crosslinked system and *Te* is the proportion of physical entanglements that is elastically active [8,38,39]. The shear modulus of this system can be determined for phantom network, affine network etc. For a phantom network, junctions can fluctuate about their mean positions because of Brownian motion and *h* has a value of one. For an affine network, these fluctuations are completely suppressed, and *h* has a value of zero. The network properties can be intermediate between these two types, in which case *h* has a value between zero and one. For Phantom network ($\mu = 2\upsilon/3$), the shear modulus becomes

(3)υ

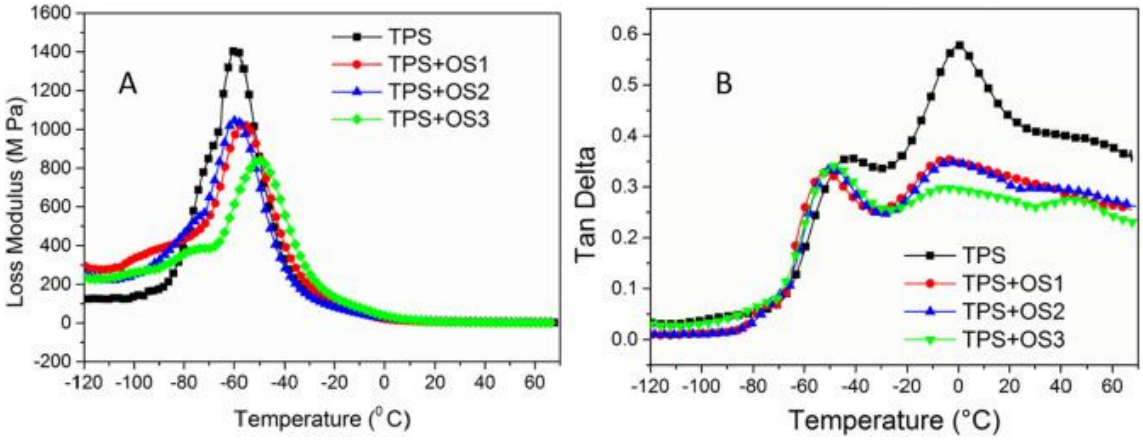

1. Download high-res image (204KB)
2. Download full-size image

Fig. 5. (A) Plot of loss modulus Vs temperature for crosslinked films. (B) Tan delta Vs temperature curve for crosslinked films.

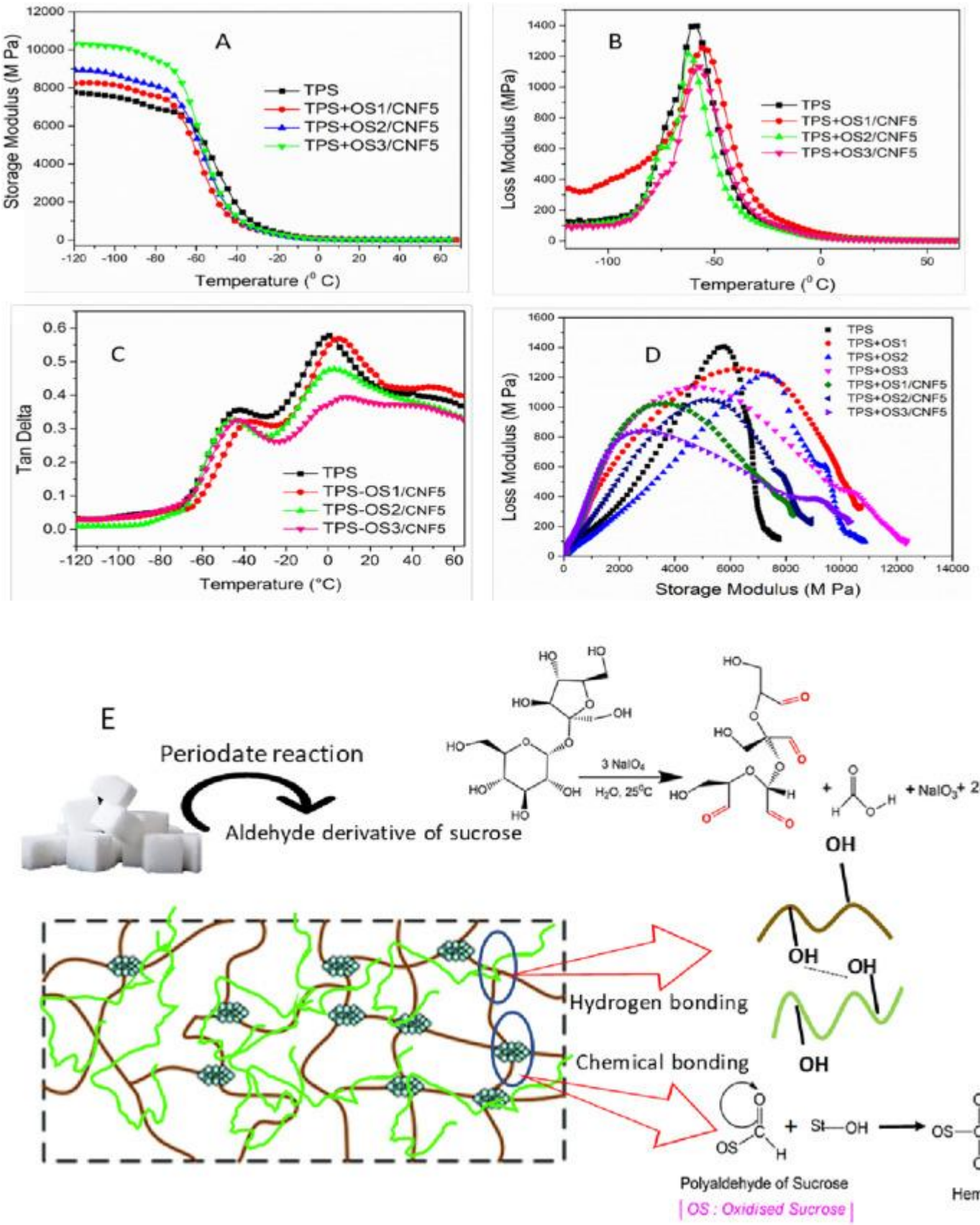

1. Download high-res image (695KB)
2. Download full-size image

Fig. 6. (A) Plot of storage modulus Vs temperature for crosslinked nanocomposite films, (B) plot of loss modulus Vs temperature for crosslinked nanocomposite films, (C) tan delta Vs

temperature for crosslinked nanocomposite films, (D) cole-cole plot, (E) schematic illustration of the crosslinking and reinforcing mechanism of oxidised sucrose and cellulose nanofibers in thermoplastic starch matrix.

Table 2. Glass transition temperature of films with calculated crosslink densities.

wt% of crosslinker	Glass transition temperature		Crosslink density (mol/m^3)	
	α_1 (glycerol rich area)	α_2 (amylopectin rich area)	Phantom model	Affine model
0	−43.1	0.1	–	–
1	−49.6	−5.2	0.064	0.021
2	−49.6	−5.1	0.074	0.025
3	−49.6	−4.8	0.077	0.031

For isotropic materials, young's modulus E can be related to the equilibrium shear modulus G as follows [8]

(4)
where n is poisons ratio which can be taken as 0.5 for elastic materials [36]. We can roughly approximate storage modulus (E^1) in the rubbery plateau (here we assume to be 0 °C) and substituting the Eq. (4) in Eq. (2). Crosslink density approximately equal to $E^{1/}RT$ for phantom network. For affine network, we perform the same calculation and crosslink density was found to be $E^1/3RT$. The values for crosslink densities were shown in Table 2.

There may be disparities in calculating the crosslink densities of the sample because of (1) eqn. for estimation of crosslink density E^1/RT is a rough approximation (2) Poisson's ratio of the sample may not be exactly 0.5, which contributes some errors in the calculation (3) intermolecular and side reactions may have taken place, resulting in an imperfect network structure [8] (4) finally the presence of plasticizer glycerol that may results in smaller crosslink density than we expect. This calculation of crosslinking density from equilibrium shear modules is valid only for amorphous networks with all elastically active network chains between crosslink points.

4.5.2. Synergistic effect of nanoreinforcement and crosslinker in the viscoelastic behaviour of starch nanocomposite

Fig. 6A shows the storage modulus Vs temperature plot of crosslinked composite reinforced with cellulose nanofibers. By closely evaluating Fig. 4, Fig. 6A, we can see that the storage modulus of the crosslinked films was higher than their corresponding nanocomposite. This might be due to the presence of nanofillers that helps to transfer stress effectively to the matrix and thereby reduces the storage modulus value. Storage modulus represents the stiffness of nanocomposite and is directly proportional to energy stored per each cycle. The loss modulus E″ is proportional to the energy dissipated during one loading cycle. The loss factor tan δ is the ratio of loss modulus to storage modulus (E″/E′). It is a measure of the energy lost, expressed in terms of the recoverable energy, and represents mechanical damping or internal friction in a viscoelastic system. A high estimation of tan δ is characteristic of a material that has a high, non-elastic strain segment, though a low esteem demonstrates one that is more flexible. In this case, derivative of sucrose was used as a crosslinker in starch-based system. Sucrose was modified via periodate cleavage which oxidises only the vicinal hydroxyl groups. As we mentioned earlier, these aldehyde group can enter into chemical bonding with hydroxyl group of the starch to form hemiacetals/acetals. The remaining hydroxyl group of the thermoplastic starch could reinforce

with cellulose nanofiber. So, we expect combined effect of crosslinking and reinforcement on the final performance of starch films (Fig. 6E).

We can see that the storage modulus value of nanocomposite is lower than that of crosslink films. Maximum storage modulus obtained for nanocomposite with 3 wt% of crosslinker oxidised sucrose (OS) is around 10×10^4 MPa and for crosslinked films without nanofiller is around 12×10^4 MPa. The temperature that corresponds to the maximum of the tan δ peak is "Tg", the glass transition temperature. This shows the importance of the glass transition as a material property. It is clear that it specifies substantial changes in the rigidity that the material experiences in a short span of temperatures.

In the case of crosslinked nanocomposites, both crosslinker and nanofiller amount play an important role in determine the glass transition temperature. As we reported earlier, in starch-cellulose nanocomposite system, cellulose exists in glycerol rich phase and at the interface. In this case we can see that the Tg of crosslink nanocomposite shifts slowly to the high temperature region upon the addition of nanofillers. These results attributed to the tendency of the cellulose to localize at the interphase.

4.5.3. Theoretical predictions of storage modulus of crosslink nanocomposites

It is important to consider that modulus of the glassy region determines the strength of intermolecular interaction and stiffness is characteristic property of the amorphous region, which is flexible above the glass transition temperature. As we discussed above, the storage modulus of the nanocomposites is greater than of pure TPS (still lower than crosslinked films Fig. 6A). This is due to the effective inclusion of nanofibers into the matrix. The storage modulus of the composite after filler dispersion can be calculated theoretically by several models like rule of mixtures, which was given by the equation,

(5)
where E_c' are E'_m respectively are the moduli of composite and matrix respectively and V_f the volume fraction of filler.

Later Einstein [40] modified the equation by including adhesion parameter and given by the equation

(6)
where 2.5 is the adhesion parameter considering system to have a good matrix/filler interaction. This model is used to investigate the adhesion between filler and matrix at low filler concentration.

Followed by Einstein model, Guth modified the equation by considering higher physical and chemical interaction between filler and matrix and modified the equation as

(7)

The experimental and theoretical values of storage moduli of crosslinked nanocomposite shown in Table 3. It can be seen that the experimental values are greater than the theoretical values determined by three models evaluated. The theoretical values are in good agreement with Guth model suggesting there must be both physical and chemical interaction between filler and matrix. It was clear that, for nanocomposite with 3 wt% crosslinker, none of the models agree with the experimental value of storage modulus. This points firmly indicate that there may be chances of aggregation of CNF nanoparticles in TPS + OS3 nanocomposite.

Table 3. Theoretical prediction of storage modulus.

Sample code	Experimental moduli (M Pa)	Rue of mixtures (M Pa)	Einstein model (M Pa)	Guth model (M Pa)	E_f
TPS + OS1/CNF 5	107.08	101.76	107.63	107.65	0.97
TPS + OS2/CNF 5	108.09	102.70	108.63	108.65	1.52
TPS + OS3/CNF 5	111.48	105.43	111.0	111.04	1.14

4.5.3.1. Effectiveness of dispersion E_f

Using the storage modulus values, we can predict different parameters like effective dispersion, degree of entanglement and reinforcing efficiency. The effectiveness of CNF addition on to starch matrix can be estimated using the following equation.

(8)

where $\mathbf{E_f}$ indicates the effectiveness of the dispersion, E_g and E_r are storage moduli at glassy and rubbery regions of the nanocomposite and the neat starch which were taken at -90^0c and 0^0C respectively [41].

4.5.4. Tan delta peak

The nature of polymeric system is one of the key factor behind the magnitude of tan δ peak height. It may be considered as a dissipation of energy due to internal friction and molecular motions. By observing Fig. 6C, we can see that by increasing the crosslinker content, the damping peak decreases. Damping peak occurs at the vicinity of glass transition area where the polymer converted from rigid to an elastic material which in association with movement of polymeric chain which are initially in a frozen stage. Upon the addition of fillers, there is the shear stress concentration at the filler surface in addition to the energy dissipation to the matrix. From the Fig. 6C, one can notice that when the crosslinker content increases, from 2 to 3 wt% there is a shift of tan delta peak to the left. This may be due to the tendency of nanoparticle to move towards the glycerol rich area. In our previous study [19], we found that there is a progressive migration of plasticizer glycerol in starch/CNF nanocomposite and thereby there is a shift of tan δ to lower temperature i.e., the glass transition temperature shifts to lower temperature rubbery region. In this case, we can notice that at higher crosslinker content, the α_1 and α_2 transition peak shits to lower temperature (Table 4). Since the reinforcing content are same for all the crosslink films, the damping height found to be unaffected (0.33) for α_1 transition. Compared to neat TPS the Tg of α_1 and α_2 transition of nanocomposite with 1 wt% of crosslinker shifts to higher temperature, which may due to the migration of plasticizer glycerol to glycerol lean area that we proposed earlier. This shift in the glass transition temperature upon CNF inclusion seems to be disagree with previous reported results of glycerol plasticized starch system reinforced with nanowhiskers and nanocrystals [35,42,43]. This disparity can be explained from the sole difference between two fillers with different morphology, where the reinforcing efficiency of whiskers and crystals are low compared to the nanofibers. Cellulose nanofibers are hairy structure in which reinforcing ability depends on two factors; formation of hydrogen bonded network over the surface of matrix and tangling effect of cellulose nanofibers.

Table 4. Glass transition temperature of composite films.

Sample code	δ max (α_1 transition)	Glass transition temperature (α_1)	δ max (α_2 transition)	Glass transition temperature (α_2)

Sample code		δ max (α_1 transition)	Glass transition temperature (α_1)	δ max (α_2 transition)	Glass transition temperature (α_2)
TPS		**0.35**	**−43.1**	**0.57**	**0.1**
Crosslinked films	**TPS + OS1**	0.33	−49.6	0.35	−5.2
	TPS + OS2	0.33	−49.6	0.34	−5.1
	TPS + OS3	0.33	−49.6	0.30	−4.8
Crosslinked nanocomposite films	**TPS + OS1/CNF5**	0.32	−40.9	0.57	2.65
	TPS + OS2/CNF5	0.30	−47.7	0.38	2.66
	TPS + OS3/CNF5	0.29	−43.0	0.48	4.22

Table 1. Melting temperature of nanocomposite films.

Sample	Melting temperature Tm (°C)
TPS	71.5
TPS + OS1	79.5
TPS + OS2	90.5
TPS + OS3	94.8
TPS + OS1/CNF5	85.0
TPS + OS2/CNF5	86.8
TPS + OS3/CNF5	92.4

But in case of particulate fillers like whiskers and crystals the tangling effect is inactive. For higher concentration of OS, the plasticizer effect is inactive and crosslinker effect and reinforcing effect will be more prominent. This increase in Tg attributed to the better crosslinking of crosslinker being used to the starch system that restricts the polymer chain mobility. In starch glycerol system, the plasticizer glycerol has more affinity towards the glycerol rich area and at the interfaces as already reported by several authors [19,44,45]. But in this case, as there is a shift of both transition peak towards the lower temperature upon the addition of nanofillers preferably due to the migration of plasticizer glycerol and cellulose nanomaterial localizes in glycerol rich area and at the interfaces.

4.5.5. Cole-cole plot

Fig. 6D shows the cole-cole plot of nanocomposite with and without nanofiller. The absence of semi-circular pattern for cole-cole indicates the presence of heterogeneous character of polymeric system. It is clear from the morphological investigation from AFM that the system is heterogeneous system. As the crosslinker content increases, more of a broaden semi-circle results. Morphological results strongly support the cole-cole analysis of nanocomposites.

4.6. Biodegradability studies

Fig. 7 shows the biodegradation studies of crosslink nanocomposite films after 30 days of incubation. Compared to neat TPS, all films show a decreased biodegradation rate. After 30 days of incubation, neat TPS loses almost 80% of its initial weight where the crosslinked films lose around 30% weight only. Also, degradation rate is very much low compared to other films. The lower biodegradation rate of crosslink films is due to the following reasons. (1) Partial

crosslinking of thermoplastic starch results to form acetal/hemiacetal by itself causes nanocomposite hardly to decompose or degrade (2) due to its hydrophobia, it lost attraction towards bacteria and decreases the biodegradation rate (3) low permeability rate of crosslink films. By closely observing the figure we could notice that upon nonreinforcement, the biodegradability rate gradually increases this is due to the presence of cellulose nanofibers. Among the crosslinked nanocomposite, higher rate of biodegradation was observed for TPS + OS1/CNF5. This is because of the lower amount of crosslinker compared to the rest of crosslink sample.

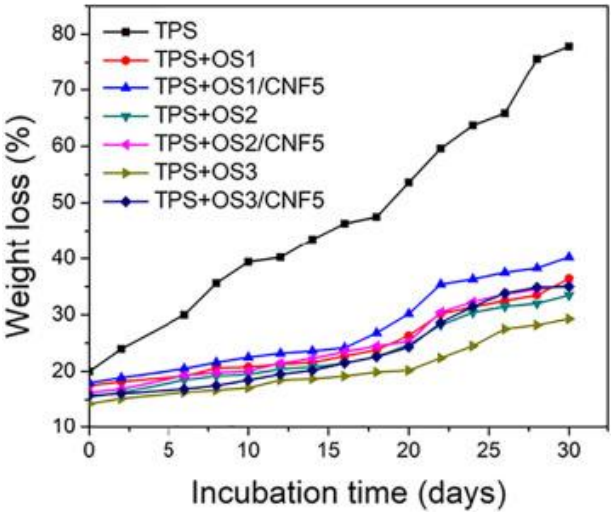

1. Download high-res image (127KB)
2. Download full-size image

Fig. 7. Biodegradation analysis of crosslink nanocomposite films.

5. Conclusions

In the present study, a bio-based disaccharide derivative, oxidised sucrose was used to crosslink starch cellulose nanocomposite films. By the addition of crosslinker the crystallinity of the crosslinked films was found to be decreased. Thermal analysis by DSC reveals than upon the addition of crosslinker the melting temperature shifts to higher temperature due to increase in crosslink density of prepared films which might result from more perfect structure, nucleation effect and the presence of crosslinks in the intercrystalline amorphous regions. The storage modulus of crosslinked films was higher than the un-crosslinked films and the Tg shifts to lower temperature. For crosslinked films without nanofiller, the damping height at glycerol rich area remains constant which indicates at that region, the plasticization effect is more prominent that effective constrained region is not formed. At the same time the damping height decreases gradually for glycerol lean area that confirms effective crosslinking. The crosslink densities are calculated using storage modulus value by applying phantom model and affine model. In general, crosslinking with a bio-based derivative and reinforcement with a nanofiller can improve the property of nanocomposite film by preserving the biodegradability.

Acknowledgement

Authors wish to acknowledge Department of Science and Technology (DST) for awarding INSPIRE (2013/888) fellowship to one of the authors. Prof. Sabu Thomas was grateful to University of Lorraine, France for Professor@lorraine honour.

References

[1]

P. Bindu, S. Thomas**Viscoelastic behavior and reinforcement mechanism in rubber nanocomposites in the vicinity of spherical nanoparticles**
J. Phys. Chem. B, 117 (2013), pp. 12632-12648, 10.1021/jp4039489
CrossRefView Record in ScopusGoogle Scholar

[2]

H. Angellier, S. Molina-Boisseau, P. Dole, A. Dufresne**Thermoplastic starch-waxy maize starch nanocrystals nanocomposites**
Biomacromolecules, 7 (2006), pp. 531-539, 10.1021/bm050797s
CrossRefView Record in ScopusGoogle Scholar

[3]

a. Cano, E. Fortunati, M. Ch??fer, J.M. Kenny, A. Chiralt, C. Gonz??lez-Mart??nez**Properties and ageing behaviour of pea starch films as affected by blend with poly(vinyl alcohol)**
Food Hydrocoll., 48 (2015), pp. 84-93, 10.1016/j.foodhyd.2015.01.008
Article
Download PDFView Record in ScopusGoogle Scholar

[4]

B. Tajeddin, R.A. Rahman, L.C. Abdulah**The effect of polyethylene glycol on the characteristics of kenaf cellulose/low-density polyethylene biocomposites**
Int. J. Biol. Macromol., 47 (2010), pp. 292-297, 10.1016/j.ijbiomac.2010.04.004
Article
Download PDFView Record in ScopusGoogle Scholar

[5]

A. Bher, I. Uysal Unalan, R. Auras, M. Rubino, C. Schvezov**Toughening of poly(lactic acid) and thermoplastic cassava starch reactive blends using graphene nanoplatelets**
Polymers (Basel), 10 (2018), p. 95, 10.3390/polym10010095
CrossRefGoogle Scholar

[6]

M.C. Condés, M.C. Añón, A. Dufresne, A.N. Mauri**Composite and nanocomposite films based on amaranth biopolymers**
Food Hydrocoll., 74 (2018), pp. 159-167, 10.1016/J.FOODHYD.2017.07.013
Article
Download PDFView Record in ScopusGoogle Scholar

[7]

S. Benali, F. Khelifa, D. Lerari, R. Mincheva, Y. Habibi, D. Lahem, M. Debliquy, P. Dubois**Supramolecular approach for efficient processing of polylactide/starch nanocomposites**
ACS Omega, 3 (2018), pp. 1069-1080, 10.1021/acsomega.7b01465
CrossRefView Record in ScopusGoogle Scholar

[8]

B. Chiou, P.E. Schoen**Effects of crosslinking on thermal and mechanical properties of polyurethanes**
J. Appl. Polym. (2001), pp. 9-12, 10.1002/app.10056
Google Scholar

[9]

B. Sreedhar, M. Sairam, D.K. Chattopadhyay, P. a S. Rathnam, D.V. Mohan Rao**Thermal, mechanical, and surface characterization of starch-poly(vinyl alcohol) blends and borax-crosslinked films**
J. Appl. Polym. Sci., 96 (2005), pp. 1313-1322, 10.1002/app.21439

CrossRefView Record in ScopusGoogle Scholar

[10]

S. Li, Y. Xia, Y. Qiu, X. Chen, S. Shi**Preparation and property of starch nanoparticles reinforced aldehyde-hydrazide covalently crosslinked PNIPAM hydrogels**
J. Appl. Polym. Sci., 135 (2018), Article 45761, 10.1002/app.45761
CrossRefGoogle Scholar

[11]

G. Coativy, N. Gautier, B. Pontoire, A. Buléon, D. Lourdin, E. Leroy**Shape memory starch-clay bionanocomposites**
Carbohydr. Polym. (2014), 10.1016/j.carbpol.2013.12.024
Google Scholar

[12]

C. Zeppa, F. Gouanvé, E. Espuche**Effect of a plasticizer on the structure of biodegradable starch/clay nanocomposites: thermal, water-sorption, and oxygen-barrier properties**
J. Appl. Polym. Sci., 112 (2009), pp. 2044-2056, 10.1002/app.29588
Article
Download PDFCrossRefView Record in ScopusGoogle Scholar

[13]

J.H.R. Llanos, C.C. Tadini**Preparation and characterization of bio-nanocomposite films based on cassava starch or chitosan, reinforced with montmorillonite or bamboo nanofibers**
Int. J. Biol. Macromol., 107 (2018), pp. 371-382, 10.1016/J.IJBIOMAC.2017.09.001
View Record in ScopusGoogle Scholar

[14]

I. Surya, N. Hayeemasae**Effects of alkanolamide addition on crosslink density, mechanical and morphological properties of chloroprene rubber compounds**
IOP Conf. Ser. Mater. Sci. Eng., 343 (2018), Article 012028, 10.1088/1757-899X/343/1/012028
Article
Download PDFGoogle Scholar

[15]

M. Valodkar, S. Thakore**Isocyanate crosslinked reactive starch nanoparticles for thermo-responsive conducting applications**
Carbohydr. Res., 345 (2010), pp. 2354-2360, 10.1016/J.CARRES.2010.08.008
View Record in ScopusGoogle Scholar

[16]

Y. Yin, J. Li, Y. Liu, Z. Li**Starch crosslinked with poly(vinyl alcohol) by boric acid**
J. Appl. Polym. Sci., 96 (2005), pp. 1394-1397, 10.1002/app.21569
Article
Download PDFCrossRefView Record in ScopusGoogle Scholar

[17]

B. Ghanbarzadeh, H. Almasi, A.a. Entezami**Improving the barrier and mechanical properties of corn starch-based edible films: effect of citric acid and carboxymethyl cellulose**
Ind. Crop. Prod., 33 (2011), pp. 229-235, 10.1016/j.indcrop.2010.10.016
View Record in ScopusGoogle Scholar

[18]

N.L. Garcia, L. Ribba, A. Dufresne, M.I. Aranguren, S. Goyanes**Physico-mechanical properties of biodegradable starch nanocomposites**
Macromol. Mater. Eng., 294 (2009), pp. 169-177, 10.1002/mame.200800271

CrossRefView Record in ScopusGoogle Scholar

[19]

P. Balakrishnan, M.S. Sreekala, M. Kunaver, M. Huskić, S. Thomas**Morphology, transport characteristics and viscoelastic polymer chain confinement in nanocomposites based on thermoplastic potato starch and cellulose nanofibers from pineapple leaf**
Carbohydr. Polym. (2017), 10.1016/j.carbpol.2017.04.017
Article
Download PDFGoogle Scholar

[20]

M.F. Butler, R.E. Cameron**A study of the molecular relaxations in solid starch using dielectric spectroscopy**
Polymer (Guildf), 41 (2000), pp. 2249-2263, 10.1016/S0032-3861(99)00366-3
View Record in ScopusGoogle Scholar

[21]

A. Dufresne**Dynamic mechanical analysis of the interphase in bacterial polyester/cellulose whiskers natural composites**
Compos. Interfaces, 7 (2000), pp. 53-67, 10.1163/156855400300183588
CrossRefView Record in ScopusGoogle Scholar

[22]

S. Veelaert, M. Polling, D. De Wit**Structural and physicochemical changes of potato starch along periodate oxidation**
Starch - Stärke, 47 (1995), pp. 263-268, 10.1002/star.19950470706
CrossRefView Record in ScopusGoogle Scholar

[23]

R. Wongsagon, S. Shobsngob, S. Varavinit**Preparation and physicochemical properties of dialdehyde tapioca starch**
STARCH - STÄRKE, 57 (2005), pp. 166-172, 10.1002/star.200400299
CrossRefView Record in ScopusGoogle Scholar

[24]

H. Xu, H. Canisag, B. Mu, Y. Yang**Robust and flexible films from 100% starch cross-linked by biobased disaccharide derivative**
ACS Sustain. Chem. Eng., 3 (2015), pp. 2631-2639, 10.1021/acssuschemeng.5b00353
CrossRefView Record in ScopusGoogle Scholar

[25]

J. Kumirska, M. Czerwicka, Z. Kaczyński, A. Bychowska, K. Brzozowski, J. Thöming, P. Stepnowski**Application of spectroscopic methods for structural analysis of chitin and chitosan**
Mar. Drugs, 8 (2010), pp. 1567-1636, 10.3390/md8051567
CrossRefView Record in ScopusGoogle Scholar

[26]

A. Mohammadi Nafchi, M. Moradpour, M. Saeidi, A.K. Alias**Thermoplastic starches: properties, challenges, and prospects**
Starch - Stärke, 65 (2013), pp. 61-72, 10.1002/star.201200201
Article
Download PDFCrossRefView Record in ScopusGoogle Scholar

[27]

J. Yu, P.R. Chang, X. Ma**The preparation and properties of dialdehyde starch and thermoplastic dialdehyde starch**
Carbohydr. Polym., 79 (2010), pp. 296-300, 10.1016/j.carbpol.2009.08.005
Article
Download PDFView Record in ScopusGoogle Scholar

[28]
Y. Zuo, W. Liu, J. Xiao, X. Zhao, Y. Zhu, Y. Wu**Preparation and characterization of dialdehyde starch by one-step acid hydrolysis and oxidation**
Int. J. Biol. Macromol., 103 (2017), pp. 1257-1264, 10.1016/j.ijbiomac.2017.05.188
Article
Download PDFView Record in ScopusGoogle Scholar

[29]
L. Goetz, A. Mathew, K. Oksman, P. Gatenholm, A.J. Ragauskas**A novel nanocomposite film prepared from crosslinked cellulosic whiskers**
Carbohydr. Polym., 75 (2009), pp. 85-89, 10.1016/J.CARBPOL.2008.06.017
View Record in ScopusGoogle Scholar

[30]
J.J.G. Van Soest, D.B. Borger**Structure and properties of compression-molded thermoplastic starch materials from normal and high-amylose maize starches**
J. Appl. Polym. Sci., 64 (1997), pp. 631-644, 10.1002/(SICI)1097-4628(19970425)64:4<631::AID-APP2>3.0.CO;2-O
Article
Download PDFCrossRefView Record in ScopusGoogle Scholar

[31]
L. Zhang, P. Liu, Y. Wang, W. Gao**Study on physico-chemical properties of dialdehyde yam starch with different aldehyde group contents**
Thermochim. Acta, 512 (2011), pp. 196-201, 10.1016/j.tca.2010.10.006
Article
Download PDFView Record in ScopusGoogle Scholar

[32]
W.A.W.A. Rahman, L.T. Sin, A.R. Rahmat, A.A. Samad**Thermal behaviour and interactions of cassava starch filled with glycerol plasticized polyvinyl alcohol blends**
Carbohydr. Polym., 81 (2010), pp. 805-810, 10.1016/j.carbpol.2010.03.052
View Record in ScopusGoogle Scholar

[33]
B. Sreedhar, M. Sairam, D.K. Chattopadhyay, P.A.S. Rathnam, D.V.M. Rao**Thermal, mechanical, and surface characterization of starch-poly(vinyl alcohol) blends and borax-crosslinked films**
J. Appl. Polym. Sci., 96 (2005), pp. 1313-1322, 10.1002/app.21439
Article
Download PDFCrossRefView Record in ScopusGoogle Scholar

[34]
A. Kaushik, M. Singh, G. Verma**Green nanocomposites based on thermoplastic starch and steam exploded cellulose nanofibrils from wheat straw**
Carbohydr. Polym., 82 (2010), pp. 337-345, 10.1016/j.carbpol.2010.04.063
View Record in ScopusGoogle Scholar

[35]
M. Neus Anglès, A. Dufresne**Plasticized starch/tunicin whiskers nanocomposites. 1. Structural analysis**
Macromolecules, 33 (2000), pp. 8344-8353, 10.1021/MA0008701
CrossRefGoogle Scholar

[36]
L.E. Nielsen, R.F. Landel, Mechanical properties of polymers and composites, M. Dekker, 1994. https://books.google.co.in/books?hl=en&lr=&id=Q-d50ibrGiUC&oi=fnd&pg=PR3&dq=Nielsen,+L.+E.+Mechanical+Properties+of+Polymers+and+Composites,+Vol.+1%3B+Marcel+Dekker:+New+York,+1974.&ots=aGtDfpT4j

7&sig=DnimzGJYo_U_AVSJzjr3UJMPIvk#v=onepage&q=Nielsen%2C L. E. Mechanical Properties of Polymers and Composites%2C Vol. 1%3B Marcel Dekker%3A New York%2C 1974.&f=false (accessed January 26, 2018).
Google Scholar

[37]
J. Queslel, J.M.- Analysis/Networks/Peptides, Undefined 1984, Molecular Interpretation of the Moduli of Elastomeric Polymer Networks of Known Structure, Springer. (n.d.). https://link.springer.com/chapter/10.1007/BFb0017103 (accessed January 26, 2018).
Google Scholar

[38]
M. Gottlieb, C.W. Macosko, G.S. Benjamin, K.O. Meyers, E.W. Merrill**Equilibrium modulus of model poly(dimethylsiloxane) networks**
Macromolecules, 14 (1981), pp. 1039-1046, 10.1021/ma50005a028
CrossRefView Record in ScopusGoogle Scholar

[39]
W.G.- Macromolecules, undefined 1975, statistical mechanics of random coil networks, ACS Publ. (n.d.). http://pubs.acs.org/doi/pdf/10.1021/ma60044a017 (accessed January 26, 2018).
Google Scholar

[40]
A. Einstein**Investigations on the Theory of Brownian Motion**
(1956)
Article
Download PDFGoogle Scholar

[41]
L.A. Pothan, Z. Oommen, S. Thomas**Dynamic mechanical analysis of banana fiber reinforced polyester composites**
Compos. Sci. Technol., 63 (2003), pp. 283-293, 10.1016/S0266-3538(02)00254-3
Article
Download PDFView Record in ScopusGoogle Scholar

[42]
W.H. Danial, Z. Abdul Majid, M.N. Mohd Muhid, S. Triwahyono, M.B. Bakar, Z. Ramli**The reuse of wastepaper for the extraction of cellulose nanocrystals**
Carbohydr. Polym., 118 (2015), pp. 165-169, 10.1016/j.carbpol.2014.10.072
View Record in ScopusGoogle Scholar

[43]
† Hélène Angellier, † Sonia Molina-Boisseau, ‡ and Patrice Dole, § Alain Dufresne*, Thermoplastic Starch–Waxy Maize Starch Nanocrystals Nanocomposites, (2006). doi:https://doi.org/10.1021/BM050797S.
Google Scholar

[44]
A. Alemdar, M. Sain**Biocomposites from wheat straw nanofibers: morphology, thermal and mechanical properties**
Compos. Sci. Technol., 68 (2008), pp. 557-565, 10.1016/j.compscitech.2007.05.044
View Record in ScopusGoogle Scholar

[45]
J. Viguié, S. Molina-Boisseau, A. Dufresne**Processing and characterization of waxy maize starch films plasticized by sorbitol and reinforced with starch nanocrystals**
Macromol. Biosci., 7 (2007), pp. 1206-1216, 10.1002/mabi.200700136
CrossRefView Record in ScopusGoogle Scholar

No articles found.

Citing articles (0)